



HAL
open science

A silicon nitride ISFET based immunosensor for tumor necrosis factor-alpha detection in saliva. A promising tool for heart failure monitoring

Hamdi Ben Halima, Francesca Bellagambi, Albert Alcacer, Pfeiffer Norman, Albert Heuberger, Marie Hangouët, Nadia Zine, Joan Bausells, Abdelhamid Elaïssari, Abdelhamid Errachid

► To cite this version:

Hamdi Ben Halima, Francesca Bellagambi, Albert Alcacer, Pfeiffer Norman, Albert Heuberger, et al.. A silicon nitride ISFET based immunosensor for tumor necrosis factor-alpha detection in saliva. A promising tool for heart failure monitoring. *Analytica Chimica Acta*, 2021, 1161, pp.338468. 10.1016/j.aca.2021.338468 . hal-03200127

HAL Id: hal-03200127

<https://hal.science/hal-03200127>

Submitted on 1 Jun 2021

HAL is a multi-disciplinary open access archive for the deposit and dissemination of scientific research documents, whether they are published or not. The documents may come from teaching and research institutions in France or abroad, or from public or private research centers.

L'archive ouverte pluridisciplinaire **HAL**, est destinée au dépôt et à la diffusion de documents scientifiques de niveau recherche, publiés ou non, émanant des établissements d'enseignement et de recherche français ou étrangers, des laboratoires publics ou privés.

1 **A silicon nitride ISFET based immunosensor for Tumor Necrosis Factor-**
2 **alpha detection in saliva. A promising tool for heart failure monitoring**

3 Hamdi Ben Halima^a, Francesca G. Bellagambi^{a,*}, Albert Alcacer^b, Norman Pfeiffer^c, Albert
4 Heuberger^d, Marie Hangouët^a, Nadia Zine^a, Joan Bausells^b, Abdelhamid Elaissari^a,
5 Abdelhamid Errachid^{a,*}

6
7
8 ^a University Claude Bernard Lyon 1, Institute of Analytical Sciences (ISA) – UMR 5280, 5 rue de la
9 Doua, 69100, Lyon, France.

10 ^b Institute of Microelectronics of Barcelona (IMB–CNM, CSIC), Campus UAB, 08193 Bellaterra,
11 Barcelona, Spain.

12 ^c Fraunhofer IIS, Fraunhofer Institute for Integrated Circuits, Am Wolfsmantel 33, 91058 Erlangen,
13 Germany.

14 ^d Information Technology (LIKE), Friedrich-Alexander-Universität Erlangen-Nürnberg (FAU), Am
15 Wolfsmantel 33, 91058 Erlangen, Germany.

16

17

18 *** Corresponding authors**

19 *E-mail address:* francesca.bellagambi@univ-lyon1.fr

20 Telephone: +33 43 74 23 569

21 ORCID iD: 0000-0002-1608-8858

22 Scopus Author iD: 55942967100

23

24 *E-mail address:* abdelhamid.errachid-el-salhi@univ-lyon1.fr

25 Telephone: +33 43 74 23 560

26 Scopus Author iD: 6602163740

27

28 **Abstract**

29 According to the European statistics, approximately 26 million patients worldwide suffer
30 from heart failure (HF), and this number seems to be steadily increasing. Inflammation plays
31 a central role in the development of HF, and the pro-inflammatory cytokine Tumor necrosis
32 factor- α (TNF- α) represents inflammation gold-standard biomarker. Early detection plays a
33 crucial role for the prognosis and treatment of HF. An Ion Sensitive Field Effect Transistor
34 (ISFET) based on silicon nitride transducer and biofunctionalized with anti-TNF- α antibody
35 for label-free detection of salivary TNF- α is proposed. Electrochemical impedance
36 spectroscopy (EIS) was used for TNF- α detection. Our ImmunoFET offered a detection limit
37 of 1 pg mL^{-1} , with an analytical reproducibility expressed by a coefficient of variance (CV)
38 resulted $< 10 \%$ for the analysis of saliva samples, and an analyte recovery of $94 \pm 6 \%$. In
39 addition, it demonstrated high selectivity when compared to other HF biomarkers such as
40 Interleukin-10, N-terminal pro B-type natriuretic peptide, and Cortisol. Finally, ImmunoFET
41 accuracy in determining the unknown concentration of TNF- α was successfully tested in
42 saliva samples by performing standard addition method. The proposed ImmunoFET showed
43 great promise as a complementary tool for biomedical application for HF monitoring by a
44 non-invasive, rapid and accurate assessment of TNF- α .

45

46

47 **Keywords**

48 Biosensor

49 ImmunoFET

50 Tumor necrosis factor- α

51 Saliva analysis

52 Electrochemical impedance spectroscopy

53 Heart failure

54 **1. Introduction**

55 Heart failure (HF) is a complex clinical syndrome caused by a wide range of cardiovascular
56 disorders, such as structural or functional abnormalities of the heart, which results in the
57 impairment of the heart ability to fill or to pump out blood may eventually lead to the clinical
58 syndrome of HF. This cardiovascular chronic disease is currently the main cause of mortality
59 and poor quality of life in western societies, affecting approximately 26 million people
60 worldwide, and its prevalence continues to rise over time, with aging of the population [1,2].
61 Since HF imposes both direct costs to healthcare systems and indirect costs to society through
62 morbidity, unpaid care costs, premature mortality and lost productivity, the estimation of
63 global economic burden of HF is not accurately feasible. Therefore, increase of the population
64 prone to HF requires a more specific and focused attention to both diagnosis and monitoring
65 of the disease, both in the interest of patients than in the better management of costs linked to
66 the spread of this disease [3,4]. In addition, patients with HF often present with signs and
67 symptoms that are often nonspecific and with a wide differential diagnosis, making diagnosis
68 by clinical presentation alone challenging that, unfortunately, can often result in delays in
69 definitive diagnosis and treatment, and such delays are linked with poor prognosis [5].
70 Therefore, additional tools to aid clinical assessment would result helpful in making an
71 accurate and prompt diagnosis, and effectively prognosticate, treat and better identify high-
72 risk subjects [6]. The detection of specific biomarkers, which are measurable biological
73 markers of a pathological process, provides information about variety biological conditions
74 whether normal or pathological, and they can also be exploited not only to diagnose HF, but
75 also to monitor the course of the therapy [7]. Among the established HF biomarkers, a raised
76 circulating level of several inflammatory cytokines has been observed due to systemic
77 inflammation that characterizes HF patients [8–10]. In particular, Tumor necrosis factor-alpha
78 (TNF- α) is a pro-inflammatory cytokine observed following cardiac stress and whose
79 dysregulation and excessive production were demonstrated implicated in the pathogenesis of
80 HF as well as to adverse effects on other organs and apparatus, as well as on coagulation and
81 immune system [11–13]. TNF- α is usually quantified in blood or plasma representing an
82 additional stress, especially for elderly. Its concentration in healthy human plasma is usually
83 less than 40 pg/mL [14,15], but its level increases up to hundreds according to HF severity
84 [16,17]. TNF- α quantification is usually carried out in blood and by immunochemical
85 methods, which provide accurate and provide rapid screening and multiple analyses, but
86 several disadvantages also due to their high cost, the requirement of qualified personnel, and
87 no possibility for real time measurement. For these reasons, biosensors are a very promising

88 alternative due to their easy to use, reduced cost, portability, and possibility of on-line
89 monitoring of biomarkers by in-situ measurements [18–20]. At the same time, the
90 concentration of TNF- α in serum is reflected by its salivary levels [21] making TNF- α an
91 ideal salivary biomarker for HF monitoring. The interest to use saliva as target matrix is due
92 to the several offers advantages offered by saliva analysis if compared to blood: an easier and
93 unobtrusively sampling (even from critical subjects such as children, elder and disabled
94 people), the suitability for the screening of a large population by passing several drawbacks
95 such as invasiveness and psychological stress (especially if repeated sampling is needed), and
96 less health risks for patients and healthcare professionals [15,22–25].
97 In this paper we presented the development of an Ion Sensitive Field Effect Transistor
98 (ISFET) based on silicon nitride transducer (Si_3N_4) and biofunctionalized for TNF- α
99 detection in saliva for HF monitoring. For this purpose, monoclonal antibody TNF- α (mAb
100 anti-TNF- α) were addressed onto the Si_3N_4 surface through covalent bonding of the aldehyde-
101 silane (11-(triethoxysilyl) undecanal) TESUD obtaining an ImmunoFET. Our device provided
102 a linear response and an adequate sensitivity for the target concentration range. Moreover,
103 ImmunoFET selectivity was proven by analyzing samples containing three other HF
104 biomarkers such as Interleukin-10 (IL-10), N-terminal pro B-type natriuretic peptide (NT-
105 proBNP), and Cortisol. Matrix effect was also properly investigated. Finally, the developed
106 ImmunoFET was used to quantify TNF- α in real saliva samples by performing the standard
107 addition method (STAM). Satisfactory results, proven by a mean accuracy of 98%, confirmed
108 that our ImmunoFET can represent a promising tool for TNF- α monitoring in saliva for HF
109 monitoring. Even if some papers already report the development of electrochemical sensors or
110 biosensors for salivary TNF- α detection [19,20,26], our device would offer an innovative and
111 promising approach based on the first time use of ISFET as sensing transducer combined with
112 electrochemical impedance spectroscopy (EIS) for saliva sample analysis.

113

114 **2. Materials and methods**

115 **2.1. Chemicals and reagents**

116 TNF- α (Cat. No. 210-TA), mAb anti-TNF- α (Cat. No. MAB610), IL-10 (Cat. No. 1064-IL),
117 sterile phosphate buffer saline solution (PBS) and PBS containing 0.1% bovine serum
118 albumin (Cat. No. RB01 and RB02, respectively) were from R&D Systems (BioTechne,
119 France). Hydrocortisone (cortisol, purity 99%, Cat. No. ab141250) was from abcam (France).
120 NT-proBNP (Cat. No. 8NT2) was from HyTest (Finland). Millipore Milli-Q nanopure water

121 (resistivity $> 18 \text{ M}\Omega \text{ cm}$) was produced by a Millipore Reagent Water System (France). 11-
122 triethoxysilyl undecanal (TESUD, 90%) was purchased from abcr (Germany). Pure ethanol
123 (purity 95.0%) and sterile phosphate buffer saline (PBS) tablets were purchased from Sigma-
124 Aldrich (France). PBS buffer used in this study was prepared by dissolving PBS tablets in the
125 nanopure water as indicated by the supplier by yielding 0.01 M phosphate buffer (pH 7.4)
126 containing 0.0027 M potassium chloride and 0.137 M sodium chloride. Epoxy resin EPO
127 TEK H70E2LC was from Epoxy Technology (France).

128

129 **2.2. Instrumentation**

130 Wire bonding was performed using Kulicke & Soffa 4523 A Digital instrument from Kulicke
131 & Soffa (Singapore). The UV/Ozone Procleaner™ (BioForce, Germany) was used in order to
132 activate the ISFET's surface by creating $-\text{OH}$ groups. The electrochemical measurements
133 were performed using a VMP3 multichannel potentiostat purchased from Biologic-EC-Lab
134 (France). Data acquisition and analysis were accomplished using EC-Lab software V11.30.

135

136 **2.3. ISFET bio-functionalization**

137 Microelectronic fabrication process for ISFET realization has been carried out at the National
138 Microelectronics Centre (CSIC) of Institute of Microelectronics of Barcelona and it is
139 described elsewhere [27]. ISFETs were bio-functionalized by the immobilization of mAb
140 anti-TNF- α onto the ISFETs surface.

141 mAb anti-TNF- α have been diluted at 0.5 mg mL^{-1} in RB01 buffer according the procedure
142 provided from the supplier. This stock solution was subsequently aliquoted and then stored at
143 $-20 \text{ }^\circ\text{C}$ until use. The $10 \text{ }\mu\text{g mL}^{-1}$ mAb anti-TNF- α standard solution needed for ISFET
144 functionalization has been obtained by further dilution of mAb mother solution in RB01 after
145 gentle defrosting at $4 \text{ }^\circ\text{C}$ for 15 min before use.

146 The bio-functionalization process was started by cleaning the ISFETs with acetone/ethanol
147 using sonicator bath; ISFETs were then thoroughly rinsed with Milli-Q water. Afterwards, the
148 device was then placed for 30 min into the UV/O₃ cleaner to activate ISFET surface by
149 creating $-\text{OH}$ groups onto the Si_3N_4 surface. Subsequently, the activated ISFETs were
150 functionalized with TESUD ((11-triethoxysilyl) undecanal) using vapor-phase method, an
151 activation process already presented by our group in which Si_3N_4 and HfO_2 surfaces have
152 been aldehyde-functionalized to detect human serum albumin [28] and salivary cortisol [29],
153 respectively

154 Then, the devices were placed into an oven at 100 °C for 1 h. After that, ISFETs were rinsed
155 with absolute ethanol and dried using nitrogen to eliminate the excess of TESUD. Next, the
156 functionalized ISFETs were incubated with mAb anti-TNF- α (10 $\mu\text{g mL}^{-1}$ in PBS). Finally,
157 the ImmunoFET was left in ethanolamine (1% v/v in PBS) for 45 min at room temperature
158 (20 ± 2 °C). This step was very important to prevent nonspecific bonding at the detection
159 stage.

160

161 **2.4. Standard solutions and saliva samples preparation**

162 TNF- α have been reconstituted at 0.1 mg mL $^{-1}$ in RB02 buffer according to the reconstitution
163 procedure provided from the supplier. This stock solution was then aliquoted and stored at
164 -20 °C until use. Before use, each aliquot (10 μL) was gently defrosted at 4 °C for 15 min and
165 then it was further diluted in PBS to obtain working standard solutions needed for both
166 calibrations in PBS (in the concentration range 1 – 50 pg mL $^{-1}$) and for spiking saliva
167 samples.

168 Standard solutions containing other HF biomarkers in PBS (e.g. IL-10, NT-proBNP, and
169 cortisol, in the concentration range 5 – 20 pg mL $^{-1}$) have been prepared in a similar way to
170 carry out the interference study.

171 Saliva has been collected from nominally healthy volunteers according to a procedure
172 described elsewhere [23,30]. Briefly, subjects were asked to freely roll a synthetic swab
173 (Salivette[®] from Sarstedt, Germany) in their mouth. Saliva was then recovered by
174 centrifugation of the swab at 7000 rpm for 5 min at 4 °C, and all samples were pooled. The
175 pooled saliva sample (PSS) was then aliquoted.

176 One aliquot (5 mL) was used for preparing calibration samples (TNF- α calibration in saliva) to
177 investigate both method linearity and matrix effect. Matrix effect was excluded by comparing,
178 at a confidence level of 95%, the slopes, reported with the corresponding standard deviation, of
179 the calibration curves obtained by analyzing TNF- α standard solutions in PBS and saliva
180 samples spiked in the same concentration range [31].

181 Another aliquot (450 μL) was analyzed by performing the STAM. To confirm the result, two
182 other aliquots (450 μL) were spiked with a known amount of TNF- α to obtain two samples
183 containing 50 and 330 pg mL $^{-1}$ respectively. These samples have been treated as *unknown*
184 *samples* and analyzed by carrying out the STAM.

185 STAM samples were prepared by adding a constant volume (50 μL) of sample to each of four
186 1.5 mL Eppendorf[®] Lo-bind centrifuge tubes (Eppendorf, France). The first tube was then

187 made up to a final volume of 1 mL by adding 950 μL of PBS, obtaining the sample C_0 .
188 Increasing volumes of a 500 ng mL^{-1} TNF- α standard solution were added to the subsequent
189 tubes and each flask was then made up to 1 mL with PBS, obtaining sample C_1 (addition of 20
190 pg mL^{-1}), sample C_2 (addition of 50 pg mL^{-1}), and sample C_3 (addition of 100 pg mL^{-1}),
191 respectively. Afterwards, SAM samples were analyzed by EIS as described in 2.5.

192

193 **2.5. EIS measurements**

194 EIS measurements have been carried out after incubation at room temperature (20 ± 2 $^\circ\text{C}$) of
195 the ImmunoFET in standard solutions, spiked saliva samples or STAM samples for 30 min
196 each, followed by PBS washing. EIS measurements were carried out in PBS, with a frequency
197 ranged from 10 KHz to 10 Hz, two frequency points per frequency decade, and using a
198 modulation voltage of 75 mV (E_{ac}). During the measurements, the potential was kept at 0 V
199 (E_{dc}) versus the Ag/AgCl reference. EIS measurements were performed at room temperature
200 (20 ± 2 $^\circ\text{C}$) and in a faraday cage to avoid electrical and luminosity interference. The
201 modeling of the obtained EIS data was achieved by the EC-Lab software using the
202 Randomize + Simplex method, stopped on 5000 iterations.

203 Data fitting on EIS spectra was achieved using an equivalent circuit model [$R_1 + Q_2/R_2$] shown
204 in Fig. 1, in which $R_1 = R_s$ and it corresponds to the resistance of the electrolyte solution (PBS);
205 Q_2 is the constant phase element (CPE) that is in parallel with R_2 , which is the charge transfer
206 resistance (R_{ct}). Curves were obtained by plotting the $\Delta R/R$ normalized data as a function of
207 TNF- α concentration. $\Delta R/R$ values have been normalized using the following equation ($R_{Ag} -$
208 R_{Ab})/ R_{Ab} , where R_{Ag} corresponds to R_2 of the antigen (TNF- α), and R_{Ab} to the R_2 of mAb anti-
209 TNF- α .

210

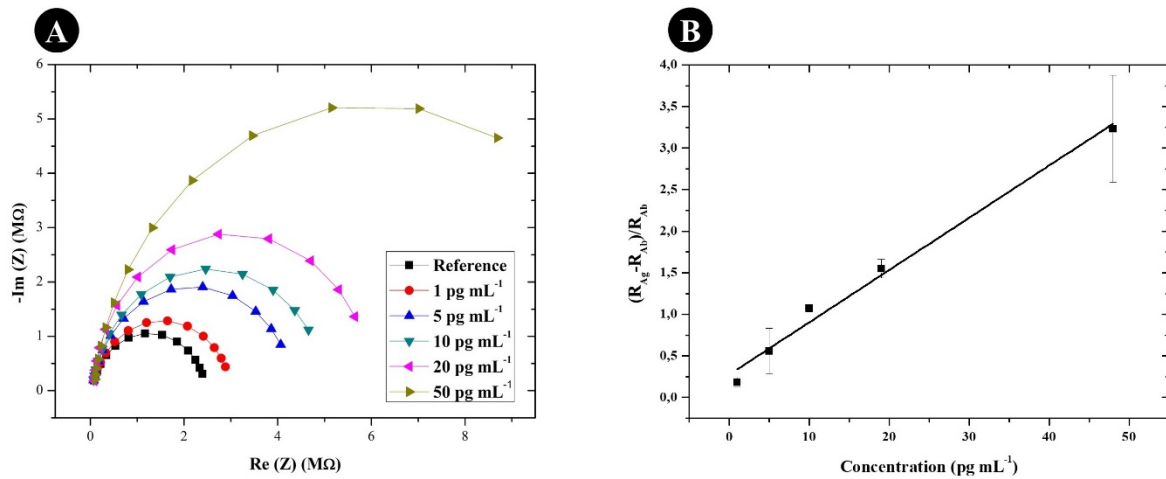
211

212 **3. Results and Discussion**

213 **3.1. Standard solution analysis**

214 Our ImmunoFET was first tested to verify the interaction between immobilized mAb anti-
215 TNF- α and recombinant human TNF- α in the concentration range from 1 to 50 pg mL^{-1} . This
216 concentration range was chosen taking into account both the dilution factor of 20 provided for
217 STAM sample preparation and the TNF- α concentration range expected in saliva collected
218 from HF patients (from few dozen up to 1000 pg mL^{-1}). Fig .1A shows the Nyquist plots
219 obtained by plotting the real part of impedance ($\text{Re}(Z)$) against the imaginary part of
220 impedance ($-\text{Im}(Z)$). The R_{ct} increased accordingly to TNF- α concentration, confirming that

221 our developed ImmunoFET was sensitive to the raise of TNF- α concentration. The increase in
 222 R_{ct} is explained by the binding of TNF- α to the mAb anti-TNF- α immobilized onto the
 223 ISFET, which produce an insulating layer that increases the R_{ct} . Then, the Nyquist plots
 224 obtained were fitted using the equivalent circuit described in 2.5 and shown in Fig. 1A, and
 225 the corresponding fitting parameters are presented in Table 1. Fig. 1B shows the related
 226 calibration curve, confirming that our ImmunoFET response is linear to TNF- α concentration,
 227 as demonstrated by R^2 equal to 0.988 ± 0.027 (CV% 2%). The calibration curve resulted $y =$
 228 $0.062 (\pm 0.011) x + 0.276 (\pm 0.011)$. The limit of detection (LOD) of our ImmunoFET was
 229 obtained from equation $3 S/m$ [32], where S is the residual standard deviation of the linear
 230 regression and m is the slope of the regression line, and resulted 1 pg mL^{-1} .
 231



232
 233 **Fig 1. (A)** Example of Nyquist plots for the equivalent circuit model obtained by analyzing TNF- α
 234 standard solutions in PBS (1; 5; 10; 20; and 50 pg mL^{-1}). EIS frequency ranged from 10 kHz to 10 Hz,
 235 with E_{ac} 75 mV and E_{dc} 0 V vs Ag/AgCl; **(B)** Calibration curve obtained by analyzing standard
 236 solution containing TNF- α in the concentration range 1 – 50 pg mL^{-1} using the ImmunoFET
 237 functionalized with mAb-TNF- α .
 238
 239
 240

241 **Table 1.** Fitting parameters obtained from the equivalent circuit model [$R_1 + Q_2/R_2$]. $R_1 = R_s$ is the resistance of
 242 the electrolyte solution; Q_2 is the constant phase element; $R_2 = R_{ct}$ is the charge transfer resistance, and χ is the
 243 error on the fit.

Concentration	$R_1(\text{k}\Omega)$	$Q_2 (\text{nF}\cdot\text{s}^{(a-1)})$	$R_2 (\text{k}\Omega)$	χ
Reference	33.270	1.339	2461	$7.318 \cdot 10^{-3}$
1 pg mL^{-1}	36.155	1.312	3004	$7.431 \cdot 10^{-3}$
5 pg mL^{-1}	39.539	1.098	4316	$5.731 \cdot 10^{-3}$
10 pg mL^{-1}	40.171	1.080	5032	$4.821 \cdot 10^{-3}$
20 pg mL^{-1}	43.680	1.058	6468	$6.216 \cdot 10^{-3}$
50 pg mL^{-1}	45.287	0.9759	11540	$3.371 \cdot 10^{-3}$

244

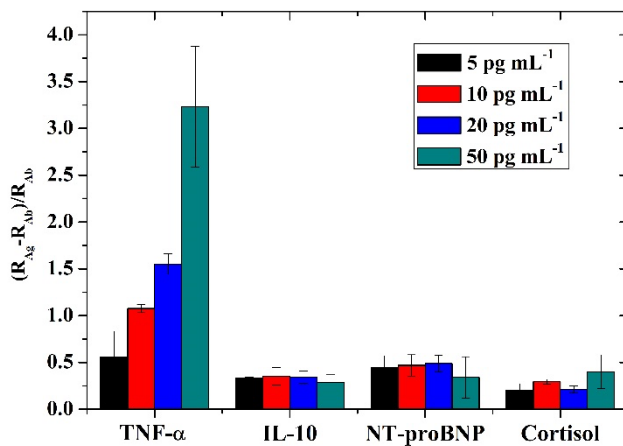
245

246 3.2. Selectivity study

247 Selectivity study was carried out by analyzing standard solutions containing TNF- α and three
248 other HF biomarkers namely IL-10, NT-proBNP, and Cortisol in order to assess the levels of
249 interferences from these biomarkers, using the same experimental conditions and concentration
250 range from 5 to 50 pg mL^{-1} . From Fig. 2, our ImmunoFET demonstrate to be highly selective
251 toward TNF- α when compared to the other three HF biomarkers. In fact, the corresponding
252 calibration curves resulted $y = 0.060x + 0.372$ ($R^2 = 0.993$) for TNF- α ; $y = -0.001x + 0.357$ (R^2
253 $= 0.813$) for IL-10; $y = -0.002x + 0.494$ ($R^2 = 0.701$) for NT-proBNP; and $y = 0.003x + 0.196$
254 ($R^2 = 0,708$) for cortisol.

255

256



257

258 **Fig 2.** Results from interference study obtained by analyzing standard solution containing TNF- α or
259 other HF biomarkers (e.g. IL-10, NT-proBNP, and Cortisol) in the concentration range 5 – 50 pg
260 mL^{-1} using the ImmunoFET functionalized with mAb-TNF- α .

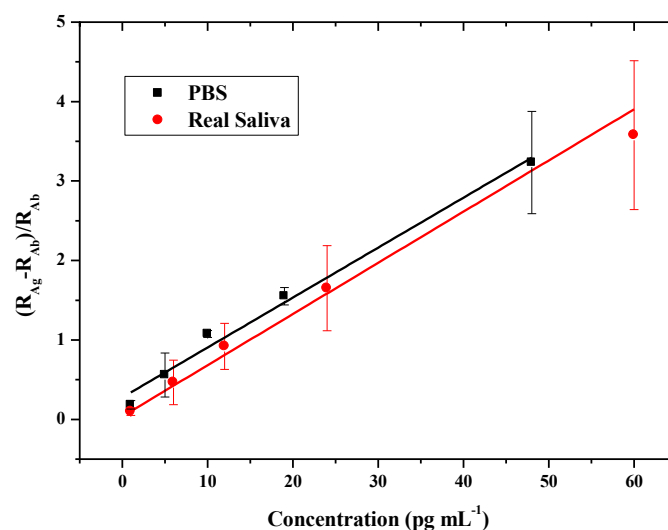
261

262 3.3. Saliva samples

263 3.3.1. Calibration in saliva sample

264 Analysis of saliva calibration samples described in 2.4. provided a calibration curve described
265 by $y = 0.058 (\pm 0.014) + 0.144 (\pm 0.130)$ and confirmed the method linearity by an R^2 equal
266 to 0.995 ± 0.002 (CV 0.2%). The presence of matrix effect was ruled out by comparing the
267 slopes of the calibration curves (i.e. PBS and spiked saliva samples) at a confidence level of
268 95%. The comparison of calibration curves in PBS and real saliva is shown in Fig. 3.

269



270

271 **Fig 3.** Comparison of calibration curves used for method linearity and matrix effect investigation that
 272 were obtained from the analysis of TNF- α standard solution in PBS (black, described by $y = 0.062 (\pm$
 273 $0.011) x + 0.276 (\pm 0.011)$ with $R^2 = 0.988 \pm 0.027$) and in spiked saliva samples (red, described by $y =$
 274 $0.058 (\pm 0.014) + 0.144 (\pm 0.130)$ with $R^2 = 0.995 \pm 0.002$), respectively.

275

276

277

278 3.3.2. TNF- α quantification in saliva samples by STAM

279 TNF- α was then quantified in three aliquots of PSS (namely Aliquot I, II, and III,
 280 respectively) by performing the standard addition method. As explained in 2.4, Aliquot I was
 281 unspiked PSS, whereas Aliquot II and Aliquot III were PSS spiked with TNF- α standard
 282 solution obtaining samples containing 50 and 330 pg mL⁻¹, respectively.

283 The corresponding curves obtained from Aliquot I (which corresponded to unspiked PSS)
 284 analysis by performing the STAM resulted linear and described by $y = 0.076 (\pm 0.019) +$
 285 $0.182 (\pm 0.053)$, with $R^2 = 0.998 (\pm 0.007)$. According to STAM procedure, the concentration
 286 of TNF- α in Aliquot I was extrapolated from the curve by multiplying for the dilution factor
 287 of 20 the absolute value on x-axis for $y = 0$. In this case, TNF- α concentration in Aliquot I
 288 resulted in 48 ± 12 pg mL⁻¹. Aliquot II analysis provided a curve described by $y = 0.013 (\pm$
 289 $0.001) x + 0.059 (\pm 0.009)$ with $R^2 = 0.995 (\pm 0.006)$ and TNF- α concentration resulted $90 \pm$
 290 11 pg mL⁻¹, whereas Aliquot III analysis provided a curve described by $y = 0.013 (\pm 0.002) x$
 291 $+ 0.253 (\pm 0.056)$, with $R^2 = 0.987 (\pm 0.007)$ and, consequently, TNF- α concentration resulted
 292 370 ± 30 pg mL⁻¹. Table 2 summarizes the results from analysis of STAM samples. Method
 293 precision, here expressed as recovery %, was evaluated by considering the bias between the
 294 expected TNF- α concentration and TNF- α calculated by extrapolation from the STAM curve,
 295 and resulted 94 ± 6 %.

296

297 **Table 2.** Data from saliva sample analysis by performing the STAM to quantify TNF- α .

Sample name	Sample type	Expected TNF- α concentration [pg mL ⁻¹]	Calculated TNF- α concentration [pg mL ⁻¹]
Aliquot I	Unspiked PSS	Unknown	48 \pm 12 pg mL ⁻¹
Aliquot II	PSS spiked with 50 pg mL ⁻¹	TNF- α concentration in Aliquot I + 50 pg mL ⁻¹	90 \pm 11 pg mL ⁻¹
Aliquot III	PSS spiked with 330 pg mL ⁻¹	TNF- α concentration in Aliquot I + 330 pg mL ⁻¹	370 \pm 30 pg mL ⁻¹

298

299

300 These data (e.g. linearity, selectivity, high precision, and LOD of 1 pg mL⁻¹) allowed to
 301 consider our ImmunoFET as a very promising tool for monitoring salivary TNF- α
 302 concentration and further tests will be carried out and implemented to confirm these results
 303 and carry out a pre-clinical study on HF patients.

304

305

306 4. Conclusions

307 Preliminary results from ImmunoFET analytical validation (e.g. linearity, selectivity, high
 308 precision, and LOD of 1 pg mL⁻¹) allowed to consider our ImmunoFET as a very promising
 309 tool for monitoring salivary TNF- α concentration. Our device also showed high selectivity
 310 towards TNF- α when compared to other HF biomarkers such as IL-10, NT-proBNP, and
 311 Cortisol. Finally, preliminary tests on TNF- α quantification saliva samples by performing the
 312 STAM proved the capacity of our ImmunoFET to determine the TNF- α concentration with a
 313 recovery almost quantitative, confirming the satisfying precision of the method. An
 314 implementation of a clinical study would fully validate our device. In fact, these results,
 315 combined with further improvements in term of accuracy and ImmunoFET integration into a
 316 LoC, can allow the monitoring of salivary levels of TNF- α confirming our ImmunoFET as a
 317 very promising tool for biomedical application such as HF monitoring by saliva analysis.

318

319 Acknowledgements

320 The authors acknowledge the financial support of the European Union's Horizon 2020
 321 research and innovation programme, Project NMBP-13-2017 KardiaTool (Grant agreement
 322 No. 768686).

323

324 **Competing interests**

325 The authors declare no competing interests.

326

327

328 **References**

- 329 [1] E.J. Benjamin, P. Muntner, A. Alonso, M.S. Bittencourt, C.W. Callaway, A.P. Carson,
330 A.M. Chamberlain, A.R. Chang, S. Cheng, S.R. Das, F.N. Delling, L. Djousse, M.S.V.
331 Elkind, J.F. Ferguson, M. Fornage, L. Chaffin Jordan, S.S. Khan, B.M. Kissela, K.L.
332 Knutson, T.W. Kwan, D.T. Lackland, T.T. Lewis, J.H. Lichtman, C.T. Longenecker, M.
333 Shane Loop, P.L. Lutsey, S.S. Martin, K. Matsushita, A.E. Moran, M.E. Mussolino, M.
334 O’Flaherty, A. Pandey, A.M. Perak, W.D. Rosamond, G.A. Roth, U.K.A. Sampson,
335 G.M. Satou, E.B. Schroeder, S.H. Shah, N.L. Spartano, A. Stokes, D.L. Tirschwell,
336 C.W. Tsao, M.P. Turakhia, L.B. VanWagner, J.T. Wilkins, S.S. Wong, S.S. Virani,;
337 American Heart Association Council on Epidemiology and Prevention Statistics
338 Committee and Stroke Statistics Subcommittee, Heart Disease and Stroke Statistics-
339 2019 Update: A Report From the American Heart Association, *Circulation*. 139 (2019)
340 e56–e528. <https://doi.org/10.1016/j.Sc.2010.00372>.
- 341 [2] S.S. Virani, A. Alonso, E.J. Benjamin, M.S. Bittencourt, C.W. Callaway, A.P. Carson,
342 A.M. Chamberlain, A.R. Chang, S.Cheng, F.N. Delling, L. Djousse, M.S.V. Elkind, J.F.
343 Ferguson, M. Fornage, S.S. Khan, B.M. Kissela, K.L. Knutson, T.W. Kwan, D.T.
344 Lackland, T.T. Lewis, J.H. Lichtman, C.T. Longenecker, M. Shane Loop, P.L. Lutsey,
345 S.S. Martin, K. Matsushita, A.E. Moran, M.E. Mussolino, A. Marma Perak, W.D.
346 Rosamond, G.A. Roth, U.K.A. Sampson, G.M. Satou, E.B. Schroeder, S.H. Shah, C.M.
347 Shay, N.L. Spartano, A. Stokes, D.L. Tirschwell, L.B. VanWagner, C.W. Tsao, and On
348 behalf of the American Heart Association Council on Epidemiology and Prevention
349 Statistics Committee and Stroke Statistics Subcommittee, Heart Disease and Stroke
350 Statistics—2020 Update: A Report From the American Heart Association, *Circulation*.
351 141 (2020) e139–e596. <https://doi.org/10.1161/CIR.0000000000000757>.
- 352 [3] W. Lesyuk, C. Kriza, P. Kolominsky-Rabas, Cost-of-illness studies in heart failure: a
353 systematic review 2004–2016, *BMC Cardiovasc. Disord*. 18 (2018) 74.
354 <https://doi.org/10.1186/s12872-018-0815-3>.
- 355 [4] A.A. Shafie, Y.P.Tan, C.H. Ng, Systematic review of economic burden of heart failure,
356 *Heart. Fail. Rev*. 29 (2018) 131–145. <https://doi.org/10.1007/s10741-017-9661-0>.
- 357 [5] A.A. Inamdar, A.C. Inamdar, Heart Failure: Diagnosis, Management and Utilization, *J.*
358 *Clin. Med*. 5 (2016) 62. <https://doi.org/10.3390/jcm5070062>.
- 359 [6] E.E. Tripoliti, T.G. Papadopoulos, G.S. Karanasiou, K.K. Naka, D.I. Fotiadis, Heart
360 failure: Diagnosis, severity estimation and prediction of adverse events through machine
361 learning techniques, *Comput. Struct. Biotechnol. J*. 15 (2016) 26–47.
362 <https://doi.org/10.1016/j.csbj.2016.11.001>.
- 363 [7] E. Braunwald, Biomarkers in Heart Failure, *N Engl J Med*. 358 (2008) 2148–2159.
364 <https://doi.org/10.1056/NEJMra0800239>.
- 365 [8] A. Yndestad, J.K. Damås, , E. Øie, E., T. Ueland, L. Gullestad, P. Aukrust, Role of
366 inflammation in the progression of heart failure, *Curr. Cardiol. Rep*. 9 (2007) 236–241.
367 <https://doi.org/10.1007/BF02938356>.
- 368 [9] L.F Shirazi, J. Bissett, F. Romeo, J.L. Mehta, Role of inflammation in heart failure,
369 *Curr. Atheroscler. Rep*. 19 (2017) 27. <https://doi.org/10.1007/s11883-017-0660-3>.
- 370 [10] C. Riehle, J. Bauersachs, Key inflammatory mechanisms underlying heart failure, *Herz*.
371 44 (2019) 96–106. <https://doi.org/10.1007/s00059-019-4785-8>.

- 372 [11] J. Holbrook, S. Lara-Reyna, H. Jarosz-Griffiths, M. McDermott, Tumour necrosis factor
373 signalling in health and disease, *F1000Res.* 8 (2019) F1000 Faculty Rev-111.
374 <https://doi.org/10.12688/f1000research.17023.1>
- 375 [12] M.J. Page, J. Bester, E. Pretorius, The inflammatory effects of TNF- α and complement
376 component 3 on coagulation, *Sci. Rep.* 8 (2018) 1812. <https://doi.org/10.1038/s41598-018-20220-8>.
- 377 [13] L. Puimège, C. Libert, Van F. Hauwermeiren, Regulation and dysregulation of tumor
378 necrosis factor receptor-1, *Cytokine Growth Factor Rev.* 25 (2014) 285–300.
379 <https://doi.org/10.1016/j.cytogfr.2014.03.004>.
- 380 [14] G. Kleiner, A. Marcuzzi, V. Zanin, L. Monasta, G. Zauli, Cytokine Levels in the Serum
381 of Healthy Subjects, *Mediators of Inflammation.* 2013 (2013) 1–6.
382 <https://doi.org/10.1155/2013/434010>.
- 383 [15] F.G. Bellagambi, T. Lomonaco, P. Salvo, F. Vivaldi, M. Hangouët, S. Ghimenti, D.
384 Biagini, F. Di Francesco, R. Fuoco, A. Errachid, Saliva sampling: Methods and devices.
385 An overview, *TrAC* 124 (2020) 115781. <https://doi.org/10.1016/j.trac.2019.115781>.
- 386 [16] Schumacher SM, Naga Prasad SV. Tumor necrosis factor- α in heart failure: an updated
387 review, *Curr. Cardiol. Rep.* 20 (2018) 117. <https://doi.org/10.1007/s11886-018-1067-7>.
- 388 [17] O.A. Segiet, A. Piecuch, L. Mielanczyk, M. Michalski, E. Nowalany-kozielska, Role of
389 interleukins in heart failure with reduced ejection fraction, *Anatol. J. Cardiol.* 22 (2019)
390 287–299. <https://doi.org/10.14744/AnatolJCardiol.2019.32748>.
- 391 [18] M. Lee, N. Zine, A. Baraket, M. Zabala, F. Campabadal, R. Caruso, M.G. Trivella, N.
392 Jaffrezic-Renault, A. Errachid, A novel biosensor based on hafnium oxide: Application
393 for early stage detection of human interleukin-10, *Sens. Actuator. B-Chem.* 175 (2012)
394 201–207. <https://doi.org/10.1016/j.snb.2012.04.090>.
- 395 [19] L. Barhoumi, A. Baraket, F.G. Bellagambi, G.S. Karanasiou, M. Ben Ali, D.I. Fotiadis,
396 J. Bausells, N. Zine, M. Sigaud, A. Errachid, A novel chronoamperometric
397 immunosensor for rapid detection of TNF- α in human saliva, *Sens. Actuator. B-Chem.*
398 266 (2018) 477–84. <https://doi.org/10.1016/j.snb.2018.03.135>.
- 399 [20] L. Barhoumi, A. Baraket, F.G. Bellagambi, F.M. Vivaldi, A. Baraket, Y. Clément, N.
400 Zine, M. Ben Ali, A. Elaissari, A. Errachid, Ultrasensitive immunosensor array for
401 TNF- α detection in artificial saliva using polymer-coated magnetic microparticles onto
402 screen-printed gold electrode, *Sensors. (Basel).* 19 (2019) E692.
403 <https://doi.org/10.3390/s19030692>.
- 404 [21] P. Gümüş, N. Nizam, D.F. Lappin, N. Buduneli, Saliva and Serum Levels of B-Cell
405 Activating Factors and Tumor Necrosis Factor- α in Patients With Periodontitis, *Journal*
406 *of Periodontology.* 85 (2014) 270–280. <https://doi.org/10.1902/jop.2013.130117>.
- 407 [22] A. Longo, A. Baraket, M. Vatteroni, N. Zine, J. Bausells, RogerFuoco, F. Di
408 Francesco, G.S. Karanasiou, D.I. Fotiadis, A. Menciassi, A. Errachid, Highly sensitive
409 electrochemical BioMEMS for TNF- α detection in human saliva: Heart Failure,
410 *Procedia Eng.* 168 (2016) 97–100. <https://doi.org/10.1016/j.proeng.2016.11.156>.
- 411 [23] F.G. Bellagambi, I. Degano, S. Ghimenti, T. Lomonaco, V. Dini, M. Romanelli, F.
412 Mastorci, A. Gemignani, P. Salvo, R. Fuoco, F. Di Francesco, Determination of salivary
413 α -amylase and cortisol in psoriatic subjects undergoing the Trier Social Stress Test,
414 *Microchem. Journal.* 136 (2018) 177–184.
415 <https://doi.org/10.1016/j.microc.2017.04.033>.
- 416 [24] S. Ghimenti, T. Lomonaco, F.G. Bellagambi, D. Biagini, P. Salvo, M.G. Trivella, M.C.
417 Scali, V. Barletta, M. Marzilli, F. Di Francesco, A. Errachid, R. Fuoco, Salivary lactate
418 and 8-isoprostaglandin F_{2 α} as potential non-invasive biomarkers for monitoring heart
419 failure: a pilot study, *Sci. Rep.* 10 (2020) 7441. <https://doi.org/10.1038/s41598-020-64112-2>.
- 420
421

- 422 [25] D. Biagini, T. Lomonaco, S. Ghimenti, J. Fusi, E. Cerri, F. De Angelis, F.G.
423 Bellagambi, C. Oger, J.M. Galano, E. Bramanti, F. Franzoni, R. Fuoco, F. Di Francesco,
424 Saliva as a non-invasive tool for monitoring oxidative stress in swimmers athletes
425 performing a VO_{2max} cycle ergometer test, *Talanta*. 216 (2020) 120979.
426 <https://doi.org/10.1016/j.talanta.2020.120979>.
- 427 [26] F.G. Bellagambi, A. Baraket, A. Longo, M. Vatteroni, N. Zine, J. Bausells, R. Fuoco, F.
428 Di Francesco, P. Salvo, G.S. Karanasiou, D.I. Fotiadis, A. Menciassi, A. Errachid,
429 Electrochemical biosensor platform for TNF- α cytokines detection in both artificial and
430 human saliva: Heart failure, *Sens. Actuator. B-Chem.* 251 (2017) 1026–1033.
431 <https://doi.org/10.1016/j.snb.2017.05.169>.
- 432 [27] D. Vozgirdaite, H. Ben Halima, F.G. Bellagambi, A. Alcacer, F. Palacio, N. Zine, J.
433 Bausells, A., A. Errachid, Development of an ImmunoFET for the detection of TNF- α
434 in saliva: application to heart failure monitoring, submitted to *Appl. Mater. Interfaces*.
- 435 [28] D. Caballero, J. Samitier, J. Bausells, A. Errachid, Direct patterning of anti-human
436 serum albumin antibodies on aldehyde-terminated silicon nitride surfaces for HSA
437 protein detection, *Small*. 5 (2009) 1531–1534. <https://doi.org/10.1002/sml.200801735>.
- 438 [29] H.B. Halima, N. Zine, J. Gallardo-Gonzalez, A.E. Aissari, M. Sigaud, A. Alcacer, J.
439 Bausells, A. Errachid, A novel cortisol biosensor based on the capacitive structure of
440 hafnium oxide: Application for heart failure monitoring, in: 2019 20th International
441 Conference on Solid-State Sensors, Actuators and Microsystems & Eurosensors
442 XXXIII (TRANSDUCERS & EUROSensors XXXIII), IEEE, Berlin, Germany,
443 2019: pp. 1067–1070. <https://doi.org/10.1109/TRANSDUCERS.2019.8808561>.
- 444 [30] T. Lomonaco, S. Ghimenti, D. Biagini, E. Bramanti, M. Onor, F.G. Bellagambi, R.
445 Fuoco, F., Di Francesco, The effect of sampling procedures on the urate and lactate
446 concentration in oral fluid, *Microchem. J.* 136 (2018) 255–262.
447 <https://doi.org/10.1016/j.microc.2017.02.032>.
- 448 [31] D. Biagini, S. Antoni, T. Lomonaco, S. Ghimenti, P. Salvo, F.G. Bellagambi, R.T.
449 Scaramuzza, M. Ciantelli, A. Cuttano, R. Fuoco, F. Di Francesco, F. Micro-extraction
450 by packed sorbent combined with UHPLC-ESI-MS/MS for the determination of
451 prostanoids and isoprostanoids in dried blood spots. *Talanta*. 206, 120236 (2020).
452 <https://doi.org/10.1016/j.talanta.2019.120236>.
- 453 [32] A. Shrivastava, V. Gupta, Methods for the determination of limit of detection and limit
454 of quantitation of the analytical methods, *Chron. Young. Sci.* 2 (2011) 21.
455 <https://doi.org/10.4103/2229-5186.79345>.